JACS
JOURNAL OF THE AMERICAN CHEMICAL SOCIETY
Article
pubs.acs.org/JACS

Folate-Based Near-Infrared Fluorescent Theranostic Gemcitabine Delivery

Zhigang Yang,[†] Jae Hong Lee,[†] Hyun Mi Jeon,[‡] Ji Hye Han,[‡] Nayoung Park,[†] Yanxia He,[†] Hyunseung Lee,[§] Kwan Soo Hong,*[,§] Chulhun Kang,*[,‡] and Jong Seung Kim*[,†]

[†]Department of Chemistry, Korea University, Seoul 136-701, Korea
[‡]The School of East-West Medical Science, Kyung Hee University, Yongin 446-701, Korea
[§]Division of MR Research, Korea Basic Science Institute, Cheongwon 363-883, Korea

Supporting Information

ABSTRACT: A series of heptamethine cyanine (**1**−**3**) derivatives bearing a carbamate ethyl disulfide group and gemcitabine, an anticancer drug, have been newly synthesized. Their disulfide bonds are readily cleaved by various thiols including glutathione, to result in a subsequent decomposition of the carbamate into amine followed by release of the active gemcitabine, which can be monitored by the fluorescence changes. In the biological experiment, prodrug **1** is preferentially up-taken by folate-positive KB cells over folate-negative A549 cells *via* receptor-mediated endocytosis to release gemcitabine causing cell death and to emit fluorescence in endoplasmic reticulum. Moreover, it is selectively accumulated in the KB cells which were treated to mice by dorsal subcutaneous injection. This drug delivery system is a new theranostic agent, wherein both therapeutic effect and drug uptake can be easily monitored at the subcellular level, by *in vivo* and *in vitro* fluorescence imaging.

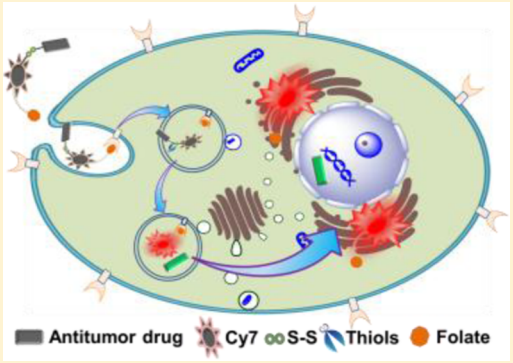

INTRODUCTION

Over the past several decades, targeted drug delivery systems (DDSs) have drawn strong attention from the chemistry and pharmacology fields.[1−4] Typically, it is composed of a prodrug and a targeting unit where they are connected through a linker, which can be cleaved by intracellular thiols,[5−7] enzymes,[8−11] or changes in pH.[12,13] The targeting unit can selectively deliver the system to a specific type of cells, for example, cancer cells *via* selective interaction with its receptor on the cell surface membrane. The crucial advantage of targeted DDS over the conventional anticancer medications is that it can release the toxic drug only when it enters the target tumor cells. However, visualization of these drug delivery processes has been hardly demonstrated since most of the antitumor drugs (e.g., gemcitabine, paclitaxel) are intrinsically nonfluorescent or weakly fluorescent. Therefore, the DDSs built with a fluorophore would allow an accurate and quantitative measurement of the drug release process, as recently demonstrated in our laboratory.[14]

To date, a number of fluorophores have been employed as reporters, such as coumarin, pyrene, 1,8-naphthalimide, xanthenes, squaraine, cyanine, borondipyrromethene difluoride, and nitrobenzofurazan.[15−17] However, several critical drawbacks were reported for most of them, including poor penetration of the excitation or emission lights through the tissues when used in animal or clinical studies.[18] In this context, a reporter with near-infrared (NIR) emission capability would be desirable for *in vivo* real-time monitoring of drug delivery. Deep tissue penetration will enhance microscopic imaging, and weak excitation energy will reduce tissue damage.

Heptamethine cyanines (Cy7s) are fluorescent dyes ideal for use in tumor imaging as they can emit light in the near-infrared (NIR) region, which is capable of deep tissue penetration and does not get affected by the autofluorescence of tissue.[19,20] The Cy7s in which the *meso*-position of its conjugation chain is occupied by amino groups exhibit a large Stokes shift, which would be advantageous in chemical sensing and biological imaging, both *in vitro* and *in vivo*.[21,22] In contrast, the Cy7 derivatives with a simple amide group reveal a rather small Stokes shift with very weak fluorescence. Therefore, considering the spectral changes upon drug delivery, designing a Cy7 derivative with an amide group that can be readily transformed into an amine group by certain intracellular reaction would be a great idea.[23]

Herein, we report a new DDS bearing Cy7 dye **1** (Scheme 1) as an NIR-based reporter. The delivery system is composed of three critical parts. A folate group is employed as a tumor-targeting ligand because its receptors are overexpressed on the surface of most cancer cells.[24−27] Second, the Cy7 unit is adopted as an NIR fluorescent reporter, in which the amide group can be rapidly decomposed into an amine group upon

Received: May 29, 2013
Published: July 18, 2013

dx.doi.org/10.1021/ja405372k | J. Am. Chem. Soc. 2013, 135, 11657−11662

Scheme 1. Chemical Structures of Target Compounds

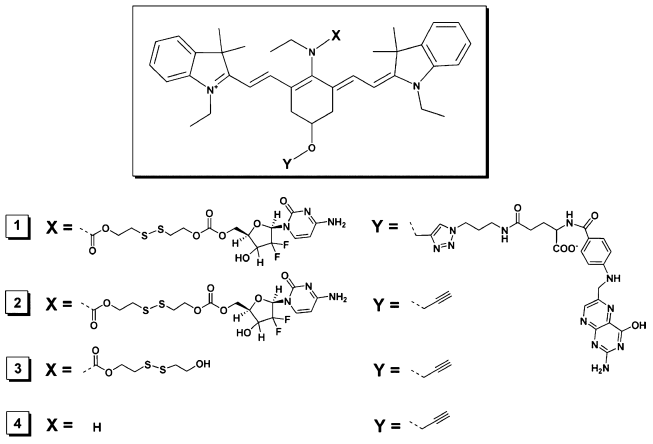

disulfide bond cleavage by intracellular thiols. Finally, gemcitabine is utilized as a model anticancer drug, which principally functions as a vigorous competitor for a pyrimidine base in the DNA replication or as an apoptosis inducer through an interaction with ribonucleotide reductase.[28] As summarized in Scheme 3, upon its reductive cleavage reaction by thiols such as L-glutathione (GSH),[7,29] the disulfide unit generates thiols, which, in turn, initiate further decomposition of the amide group and gemcitabine; simultaneously, the intensity of Cy7 fluorescence is enhanced. Thereby, **1** would have the potential to localize into the tumor cells and to deliver gemcitabine, which could be fully monitored by *in vitro* and *in vivo* real-time fluorescence imaging.

RESULTS AND DISCUSSION

For the achievement of drug delivery with the NIR fluorescent system, we first designed and synthesized a novel Cy7 dye (**5**) with a propargyloxy group at the cyclohexyl position (Schemes 2 and S1). 1,4-Cyclohexanediol was used as the starting material to react with propargyl bromide to provide 4-proparyloxycyclohexanol (**8**). **8** was then oxidized by pyridinium chlorochromate (PCC) to obtain 4-proparyloxycyclohexanone (**7**) which subsequently generated the intermediate **6** in the presence of DMF and $POCl_3$ (Vilsmeier–Haack reaction). The intermediate **6** and 1-ethyl-2,3,3-trimethyl-3*H*-indolenium iodide salt were heated in acetic anhydride to obtain a new Cy7 dye (**5**) in a 65% yield. And then, the chloro group at the *meso*-position of **5** was substituted by ethylamine to give **4** (80%). Compound **4** was subsequently reacted with phosgene and 2,2′-hydroxyethyl disulfide to produce **3**, which was further reacted with phosgene and gemcitabine to generate **2**. Compound **2** could be conjugated with 3-azidopropyl-folate (**10**) *via* a click reaction to give the prodrug **1**; the 3-azidopropyl-folate (**10**) was prepared by coupling of the folic acid and 3-azidopropylamine. All the detailed procedures, characterization, and HPLC results of the compounds have been shown in the Supporting Information.

In order to verify the spectral changes of target compounds after the carbamate decomposition at the central position of the conjugated chain of the Cy7 derivative, the spectral changes of the theranostic prodrug **1** upon its reaction with thiol-containing molecules, including GSH, are investigated and represented in Figure 1. The disulfide bond is known to be rapidly cleaved by thiols.[7,30] The prodrug **1** herein demonstrates drastic responses in the colorimetric and fluorescence

Scheme 2. Synthesis of Targeting Compounds[a]

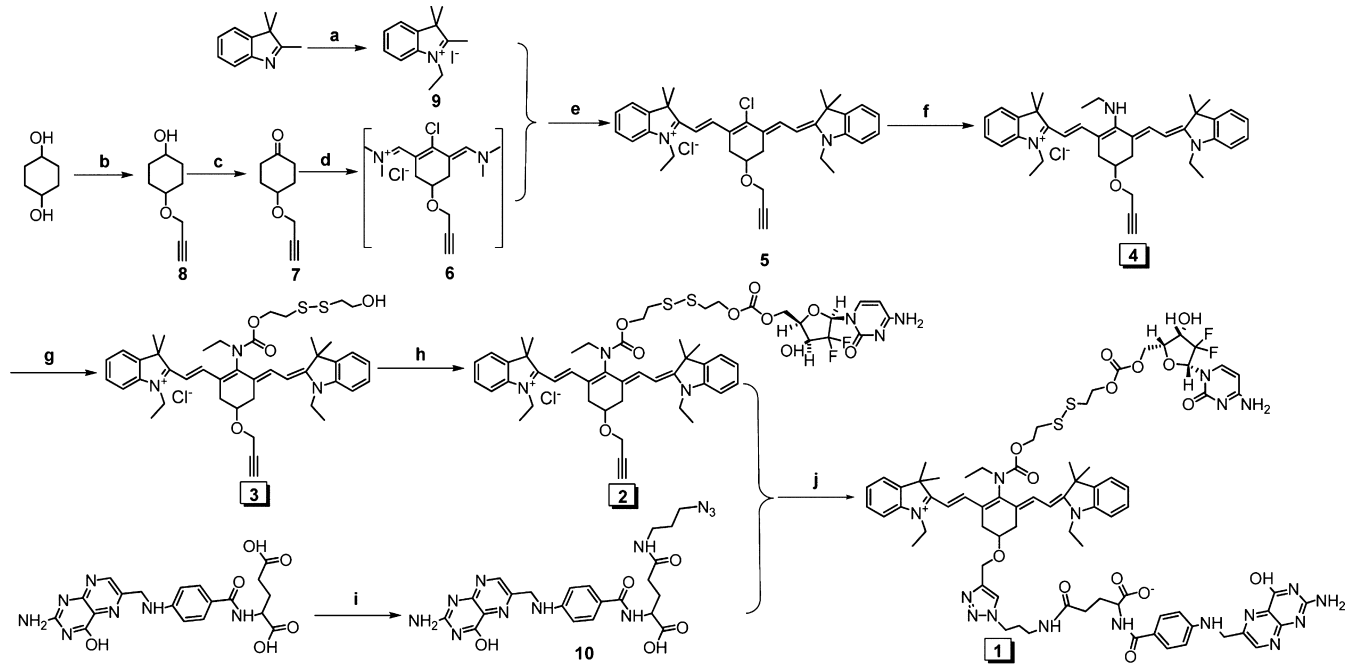

[a](a) Ethyl iodide, toluene, refluxed for 12 h, 79.6%; (b) NaH, propargyl bromide, DMF, rt, stirred overnight, 70%; (c) PCC, methylene chloride (MC), rt, stirred for 5 h, 95%; (d) DMF, $POCl_3$, 60°C, 3 h, ca. 75%; (e) anhydrous NaOAc, acetic anhydride, 100 °C, 1 h, 65%; (f) ethylamine in THF, acetonitrile, 50 °C, 80%; (g) phosgene in toluene, DIPEA, 2-(2-hydroxyethyl)disulfide in DMF, MC, rt, ca. 10%; (h) phosgene in toluene, DIPEA, DMAP, Gemcitabine in DMF, MC, rt, 63.5%; (i) 3-azidopropylamine, HATU, DMAP, DIPEA, DMF, rt, overnight, 36%; (j) $Cu(ClO_4)_2$, soduim L-ascorbate, DIPEA, 3-azidopropyl-folate, DMF, rt, 22.3%.

dx.doi.org/10.1021/ja405372k | J. Am. Chem. Soc. 2013, 135, 11657–11662

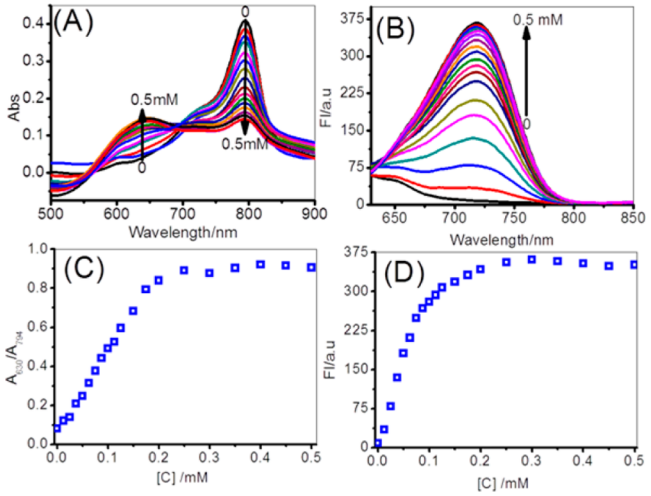

Figure 1. Absorption (A) and fluorescence (B) spectral changes of prodrug **1** (4.0 μM) in the presence of GSH in DMSO-PBS solution (10 mM, pH = 7.4) (50:50, v/v) at room temperature, λ_{ex} = 615 nm and slit width = 5, 10; and the plot of A_{630}/A_{794} (C) or I_{735} (D) vs GSH concentration; all the data were obtained after the incubation of samples for 2 h under room temperature.

spectroscopies to GSH in mixed solvents (DMSO−PBS; v/v 50%, pH = 7.4). Upon reacting with GSH, the absorption of **1** at 794 nm decreased, and a new peak concomitantly appeared at 630 nm with marked colorimetric changes (Figure 1A). The gradual increase in the absorption ratio (A_{630}/A_{794}) finally produced a plateau with GSH concentrations over 0.2 mM (Figure 1C), and the emission intensity of Cy7 (735 nm) enhanced 42-fold with good linearity (Figure 1B and 1D). These results are in harmony with the drug release model demonstrated in Scheme 2. Upon cleavage of its disulfide bond with GSH, sulfide anions are generated, which initiate the intramolecular cyclization of the carbamates at the *meso*-position of Cy7 and at the 5′-hydroxyl group of gemcitabine, inducing fluorescence by spectral changes in Cy7[31] and the gemcitabine released. And the drug release upon reaction of prodrug **1** with GSH was further identified by ESI-MS spectroscopy where we obviously observed MS peak *m*/*e*: $[M_1 + H]$ = 264.05, and $[M_2 + Na]$ = 1119.75, $[M_2 + Na + H]/2$ = 560.40 corresponding to the gemcitabine released and folate-Cy7 fragment, respectively (Figure S2 and Scheme 3). The above results lead us to confirm that active Gemcitabine was released, by concomitantly marked spectral changes of Cy7, after the disulfide bond cleavage upon GSH treatment.

Not only dual spectral changes of prodrug **1** upon incubating with various thiols were observed, the reference compound **2** without a folate group also exhibited marked colorimetric absorption and dramatic fluorescence switched-on.

For further characterization of the spectral properties of **1**, the references **3** and **4** were prepared and subjected to a calculation through the Gaussian 09 software suite[32] (Figures S3−S4). The absorption and emission bands at 628 and 724 nm for **4**, and at 785 and 794 nm for **3** in methanol, indicate that **4** produces a much larger Stokes shift (by 96 nm) than **3** (by only 9 nm). This marked Stokes shift is ascribed to the ethylamine group at the *meso*-position of the polymethine chain. In the ground state, the electron density is mainly distributed on the Cy7 backbone, excluding the centrally positioned amine. However, upon excitation, the charge is transferred from the polymethine chain to ethylamine to generate increased electron density on the nitrogen atom. Then, the amino group undergoes a change in its configuration to consume some excited energy before liberating the fluorescence of a much longer wavelength, causing a large Stokes shift. The carbamate group at the central position of the conjugating chain of reference **3** is unable to donate electrons in the ground state, and therefore, it exhibits a similar electronic distribution at both the ground and first excited states, which mainly localize at the polymethine chain. This induces a small Stokes shift. Therefore, when **3** is treated with various thiols in aqueous solution (Figures S5−S8), the carbamate at the *meso*-position of the conjugated chain could be decomposed into the amine, resulting in a change in the colorimetric absorption at 785 nm (oscillator strength f = 2.32) and 628 nm (f = 2.11), with an isosbestic point at 668 nm, demonstrating a linear relationship between A_{628}/A_{785} vs the concentration of thiols (0−0.2 mM). In addition, for prodrug **1**, the fluorescence at 724 nm (f = 2.45) was 37-fold higher compared to that at 794 nm (f = 2.55, Φ_f < 0.01), resulting in an increase in the Stokes shift (96 nm in methanol), and in turn, the fluorescence was switched on.

The disulfide bond of Cy7 dye can be selectively cleaved by thiol-containing molecules to give diverse spectral changes. When **2** or **3** was incubated with various nonthiol amino acids and metal ions, their absorption and emission spectra were hardly changed (Figures 2A, B, S9, and S10). However, upon

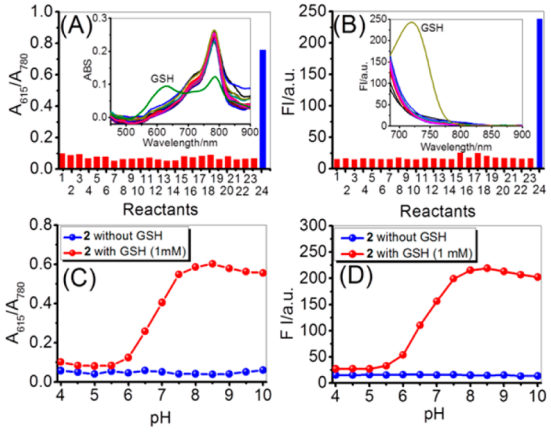

Figure 2. Changes in the absorption ratio (A) and fluorescence (B) of **2** (2.0 μM) upon addition of various reactants in PBS solution (10 mM, pH = 7.4); 1, blank; 2, Arg; 3, Phe; 4, Asp; 5, Met; 6, Ser; 7, Tau; 8, Ala; 9, His; 10, Pro; 11, Gly; 12, Leu; 13, Asn; 14, Thr; 15, Val; 16, Lys; 17, Trp; 18, Glu; 19, Ile; 20, Ca^{2+}; 21, Zn^{2+}; 22, Mg^{2+}; 23, Fe^{2+}; 24, GSH; inset, absorption (A) and fluorescence (B) spectral changes of **2** with addition of GSH (0.25 mM), other amino acids (1.0 mM), and some metal ions; and C and D, the response of **2** (2.0 μM) to the variations in pH (4.0−10.0) in the presence and absence of GSH (1.0 mM); (C) the absorbance ratio at two peaks vs pH; (D) fluorescence change vs varying pH of the solutions (DMSO−water, 10:90, v/v), λ_{ex} = 615 nm (incubation for 2 h under room temperature).

the addition of GSH (1.0 mM) at pH > 6, both absorption ratios (A_{615}/A_{780}) and fluorescence intensities of **2** and **3** increased (Figures 2C, D and S11). A slight decrease in the fluorescence intensity at pH > 8.5 may be attributed to the instability of Cy7 under such alkaline conditions. Besides, **4** is stable enough to maintain >95% of its fluorescence intensity for 60 min at 37 °C (pH = 7.4, PBS buffer; Figure S12). To investigate the DDS dynamics, a time-course experiment was

dx.doi.org/10.1021/ja405372k | J. Am. Chem. Soc. 2013, 135, 11657−11662

conducted, and the results are shown in Figures S13 and S14. The prodrug **1** incubated with various concentrations of GSH in DMSO−PBS (v/v, 50%) at 37 °C completed the disulfide cleavage reaction in 15 min to give rise to enhanced fluorescence. Therefore, it is noticeable that the compounds are stable under physiological pH (7.4) and that their fluorogenic reactions are selective to the thiol species (GSH) in the cells, which proves them to be adequate for further use in biological systems *in vitro* and *in vivo*.

To gain insight into the drug release action of **1** in the cells, we investigated whether the folate moiety can guide the probe preferentially to folate receptor-positive tumor cells or folate receptor-negative tumor cells.[33] For this, prodrug **1** was incubated with folate receptor-positive KB cells and folate receptor-negative A549 cells. As shown in Figures 3 and S15,

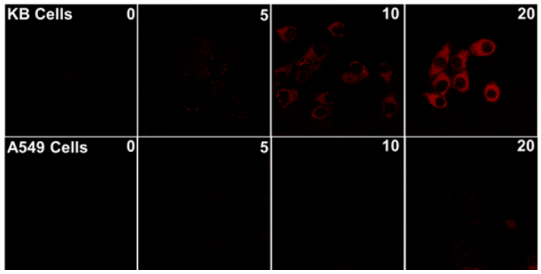

Figure 3. Confocal microscopy images of KB and A549 cells treated with prodrug **1** (1.0 μM) at various times (0, 5, 10, and 20 min); the fluorescent images were obtained via a Leica Confocal Laser Microscope (Leica TCS SP2); excited at 633 nm and detected at 650−750 nm (scale bars = 20 μm).

the KB cells exhibit strong fluorescence intensity within 20 min of incubation with prodrug **1** (1.0 μM), whereas the A549 cells showed little fluorescence signal under similar experimental condition whereas the difference in the fluorescence intensity decreased gradually with a longer incubation (Figure S16). As a result, it can be concluded that prodrug **1** can enter the cells aided by the interaction of its folate moiety with a folate receptor on the tumor cells, possibly *via* receptor-mediated endocytosis.

To provide further evidence for thiol-induced disulfide bond cleavage and concomitant fluorescence-*On*, fluorescence emission from probe **1** was studied in the presence of a strong thiol reacting agent, *N*-ethylmalemide (NEM); the results are shown in Figure S17. The fluorescence intensity of **1** in the cells decreased as the concentration of NEM increased (0−1.0 mM), reconfirming that the fluorescence enhancement of **1** is mainly triggered by intracellular thiols, as depicted in Scheme 3.

To identify the intracellular location of gemcitabine release by the theranostic prodrug **1**, colocalization experiments were carried out using confocal laser microscopy, and the results are shown in Figure 4. Both Lyso-sensor Blue DND-167 (A) and

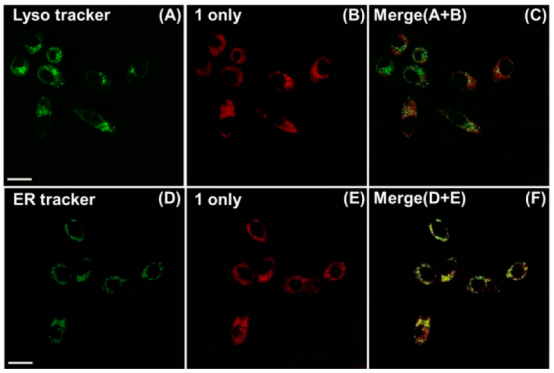

Figure 4. Confocal laser fluorescence microscopy images of KB cells with prodrug **1** and Lyso-Sensor Blue DND-167 (1.0 μM) or ER-tracker Red (0.5 μM). (A) is the image of Lyso-Sensor Blue DND-167, collected by a 370−550 nm filter upon excitation at 740 nm (two-photon excitation); (D) is the image from ER-tracker Red (0.5 μM), collected by a 530−570 nm band path filter with excitation at 514 nm; the images of the cells treated with prodrug **1** (1.0 μM) excited at 633 nm acquired by a 650−750 nm filter are shown in (B) and (E), and the merged images are shown in (C) and (F) (scale bar = 20 μm).

ER-tracker Red (D) can be visualized in green, and the probe (B and E), in red. The yellow area in the merged images (C) and (F) implicates the location where the probe and organelle selective trackers coexist. From the merged images, it is clearly noticeable that the yellow region of (F) is predominant compared to that of (C). In addition, in a parallel experiment with Mito-tracker Green FM, the merged image failed to show an intensely yellow image as in the case with ER-tracker Red (Figure S18). Therefore, it is noteworthy that thiol-induced disulfide cleavage of **1** occurred in the endoplasmic reticulum (ER), resulting in the release of gemcitabine, which presumably diffuses into the cell nucleus where it replaces one of the building blocks of nucleic acids, cytidine, during DNA replication. This process leads to forming a faulty nucleoside, leading to apoptosis.[28]

A cell viability experiment was performed to understand the cytotoxicity profile of the prodrug **1**. As demonstrated in Figure

Scheme 3. Drug (Gemcitabine) Release from the DDS by Treatment of GSH and Fluorescence Switching-on of Cy7

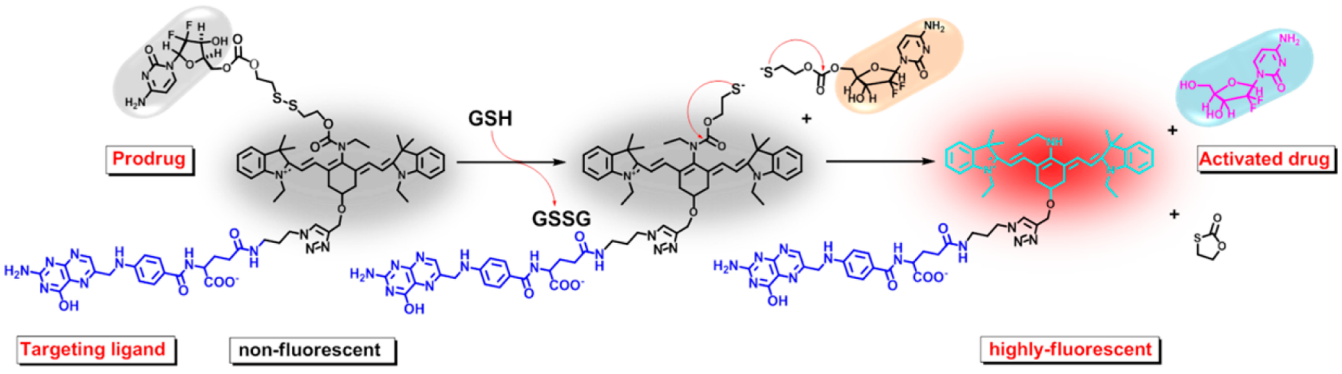

dx.doi.org/10.1021/ja405372k | J. Am. Chem. Soc. 2013, 135, 11657−11662

5, **1** and **2** are independently applied to KB and A549 cells. The cytotoxicity of **1** prefers KB cells to A549 cells whereas a

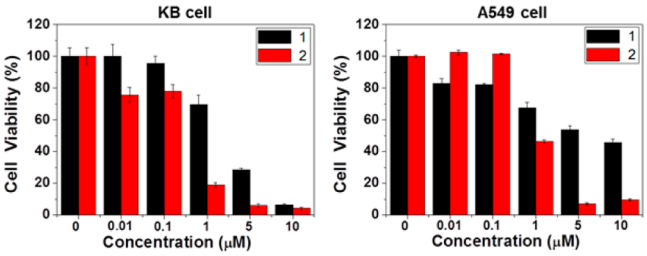

Figure 5. Cell viability assay of **1** and **2** in KB and A459 cell lines, respectively; all compounds were incubated with the cells for 72 h, and the cell viability was observed *via* MTT assay.

parallel experiment using probe **2** shows high toxicity but no preference to the cell type (Figure S19). The difference in the drug sensitivity of these cells under the prodrug **1** treatment is obviously due to the presence of the folate receptors on the KB tumor cells. However, compared to **1**, the KB cells are somehow susceptible to **2**. It seems to be delivered *via* simple diffusion which is more efficient than **1**'s delivery without any cell preference. Nonetheless, together with the results described in Figure 3, it is confirmed that the folate moiety is able to guide the prodrug **1** to the folate receptor positive KB tumor cells, followed by receptor-mediated endocytosis, resulting in apoptosis by gemcitabine drug delivery.

The fluorescent switching-on of prodrug **1** has been examined after intravenous injection of the prodrug into the xenograft tumor animal model. Tumor-bearing mice were prepared by subcutaneous injection of KB and A549 (3×10^6 each) cells into the right and left back of the mice ($n = 3$ each). After 10 days of tumor inoculation, 0.1 mM/kg (DMSO:PBS = 50:50) of prodrug **1** was administered *via* the tail vein and tumors were dissected from the mice after 24 h. Fluorescence images of cryo-sectioned tumor tissues of 7-μm thickness were obtained with excitation of Cy7 at 710/775 nm (Figure 6). Fluorescence signals in the tumor site were detected only in tissues bearing the KB tumor cells (about 1 cell per several 10^4 μm^2 tissue sections), implying that the prodrug **1** shows the tumor-targeting potential *in vivo*, which enables **1** to

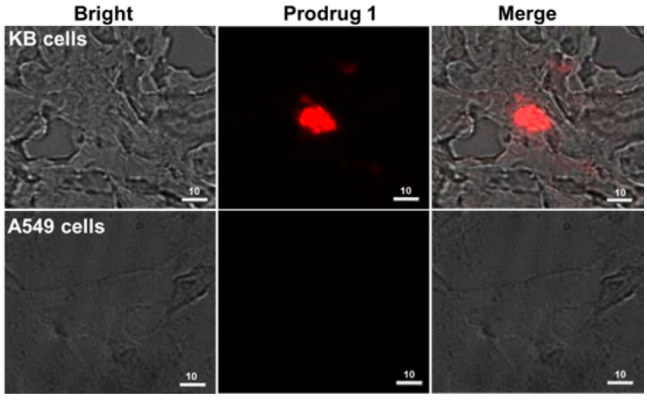

Figure 6. Fluorescence images in a tumor tissue section from KB and A549 tumor-bearing mice at 24 h postinjection of the prodrug **1** at 0.1 mM/kg; the fluorescence images were obtained by using a Deltavision RT (Applied Precision Technologies, Issaquah, WA, USA), excited at 710/775 nm, and detected at 810/890 nm (scale bar = 10 μm).

successfully deliver the gemcitabine into KB tumor cells in living mice.

CONCLUSIONS

In conclusion, a novel NIR DDS composed of three distinctive parts has been developed: a folate moiety for targeting tumor cells with folate receptors, a nonfluorescent model drug gemcitabine, and a Cy7 dye conjugated with a cleavable disulfide unit employed as a signaling reporter. The carbamate group of the prodrug **1** is decomposed into an amine upon reacting with various thiols to give marked absorption changes and enhanced fluorescence intensity. This prodrug exhibits selective cytotoxicity toward folate-positive KB cells over folate-negative A549 cells. We also found that the prodrug **1** is mainly located in the ER of the cells and that the drug was delivered upon reaction with cellular thiols. Furthermore, in vivo fluorescence imaging experimentation upon intravenous injection of the prodrug into the mice tail confirms that the prodrug **1** is selectively taken up by KB over A549 tumor tissue and its active gemcitabine is safely released. Therefore, our NIR DDS could provide a powerful new strategy for tumor targeted drug delivery, which can be easily monitored by cellular and tissue fluorescence imaging.

ASSOCIATED CONTENT

Supporting Information

Experimental details; synthesis and characteristic data (^{1}H NMR, ^{13}C NMR, mass spectra); fluorescence spectra; CLSM and HPLC data. This material is available free of charge via the Internet at http://pubs.acs.org.

AUTHOR INFORMATION

Corresponding Author

jongskim@korea.ac.kr (J.S.K.); kangch@khu.ac.kr (C.K.); kshong@kbsi.re.kr (K.S.H.)

Notes

The authors declare no competing financial interest.

ACKNOWLEDGMENTS

This work was supported by the CRI project (J.S.K., 2009-0081566) of NRF, a grant from Korea Basic Science Institute (K.S.H., D33400), and the "Cooperative Research Program for Agriculture Science & Technology Development (Project No. PJ008959)" Rural Development Administration, Republic of Korea.

REFERENCES

(1) Bildstein, L.; Dubernet, C.; Couvreur, P. *Adv. Drug Delivery Rev.* **2011**, *63*, 3−23.
(2) Kratz, F.; Müller, I. A.; Ryppa, C.; Warnecke, A. *Chem. Med. Chem.* **2008**, *3*, 20−53.
(3) Huang, C. K.; Lo, C. L.; Chen, H. H.; Hsiue, G. H. *Adv. Funct. Mater.* **2007**, *17*, 2291−2297.
(4) Kim, K.; Lee, M.; Park, H.; Kim, J.-H.; Kim, S.; Chung, H.; Choi, K.; Kim, I.-S.; Seong, B. L.; Kwon, I. C. *J. Am. Chem. Soc.* **2006**, *128*, 3490−3491.
(5) Lee, M. H.; Han, J. H.; Kwon, P.-S.; Bhuniya, S.; Kim, J. Y.; Sessler, J. L.; Kang, C.; Kim, J. S. *J. Am. Chem. Soc.* **2012**, *134*, 1316−1322.
(6) Santra, S.; Kaittanis, C.; Santiesteban, Q. J.; Perz, J. M. *J. Am. Chem. Soc.* **2011**, *133*, 16680−16688.
(7) Lee, M. H.; Yang, Z.; Lim, C. W.; Lee, Y. H.; Dongbang, S.; Kang, C.; Kim, J. S. *Chem. Rev.* **2013**, *113*, 5071−5109.

(8) Lee, M. H.; Han, J. H.; Lee, J.-H.; Choi, H. G.; Kang, C.; Kim, J. S. *J. Am. Chem. Soc.* **2012**, *134*, 17314−17319.
(9) Piggott, A. M.; Karuso, P. *Anal. Chem.* **2007**, *79*, 8769−8773.
(10) Shi, H.; Kwok, R. T. K.; Liu, J.; Xing, B.; Tang, B. Z.; Liu, B. *J. Am. Chem. Soc.* **2012**, *134*, 17972−17981.
(11) Legigan, T.; Clarhaut, J.; Opalinski, I. T.; Monvoisin, A.; Renoux, B.; Thomas, M.; Pape, A. L.; Lerondel, S.; Papot, S. *Angew. Chem., Int. Ed.* **2012**, *51*, 11606−11610.
(12) Li, Y.; Xiao, W.; Xiao, K.; Berti, L.; Luo, J.; Tsent, H. P.; Fung, G.; Lam, K. S. *Angew. Chem., Int. Ed.* **2012**, *51*, 2864−2869.
(13) Mahammud, F.; Guo, M.; Qi, W.; Sun, F.; Wang, A.; Guo, Y.; Zhu, G. *J. Am. Chem. Soc.* **2011**, *133*, 8778−8781.
(14) Lee, M. H.; Kim, J. Y.; Han, J. H.; Bhuniya, S.; Sessler, J. L.; Kang, C.; Kim, J. S. *J. Am. Chem. Soc.* **2012**, *134*, 12668−12674.
(15) Chen, X.; Pradhan, T.; Wang, F.; Kim, J. S.; Yoon, J. *Chem. Rev.* **2012**, *112*, 1910−1956.
(16) Guo, Z.; Song, N. R.; Moon, J. H.; Kim, M.; Jun, E. J.; Choi, J.; Lee, J. Y.; Bielawski, C. W.; Sessler, J. L.; Yoon, J. *J. Am. Chem. Soc.* **2012**, *134*, 17846−17849.
(17) Song, N. R.; Moon, J. H.; Jun, E. J.; Choi, J.; Kim, Y.; Kim, S.-J.; Lee, J. Y.; Yoon, J. *Chem. Sci.* **2013**, *4*, 1765−1771.
(18) Weinstain, R.; Sègal, E.; Satchi-Fainaro, R.; Shabat, D. *Chem. Commun.* **2010**, *46*, 553−555.
(19) Wang, L.; Zhu, X.; Xie, C.; Ding, N.; Weng, X.; Lu, W.; Wei, X.; Li, C. *Chem. Commun.* **2012**, *48*, 11677−11679.
(20) Lee, H.; Akers, W.; Bhushan, K.; Bloch, S.; Sudlow, G.; Tang, R.; Achilefu, S. *Bioconjugate Chem.* **2011**, *22*, 777−784.
(21) Peng, X.; Yang, Z.; Wang, J.; Fan, J.; He, Y.; Song, F.; Wang, B.; Sun, S.; Qu, J.; Qi, J.; Yan, M. *J. Am. Chem. Soc.* **2011**, *133*, 6626−6635.
(22) Peng, X.; Song, F.; Lu, E.; Wang, Y.; Zhou, W.; Fan, J.; Gao, Y. *J. Am. Chem. Soc.* **2005**, *127*, 4170−4171.
(23) Kiyose, K.; Aizawa, S.; Sasaki, E.; Kojima, H.; Hanaoka, K.; Terai, T.; Urano, Y.; Nagano, T. *Chem.—Eur. J.* **2009**, *15*, 9191−9200.
(24) Lu, Y.; Low, P. S. *J. Controlled Release* **2003**, *91*, 17−29.
(25) Yoo, H. S.; Park, T. G. *J. Controlled Release* **2004**, *100*, 247−256.
(26) Nakamura, J.; Nakajima, N.; Matsumura, K.; Hyon, S.-H. *J. Nanomedic. Nanotechnol.* **2011**, *2*, 106−109.
(27) Low, P. S.; Henne, W. A.; Doorneweerd, D. D. *Acc. Chem. Res.* **2008**, *41*, 120−129.
(28) Cerqueira, N. M. F. S. A.; Fernandes, P. A.; Ramos, M. J. *Chem.—Eur. J.* **2007**, *13*, 8507−8515.
(29) Hwang, C.; Sinskey, A. J.; Lodish, H. F. *Science* **1992**, *257*, 1496−1502.
(30) West, K. R.; Otto, S. *Curr. Drug Discovery Technol.* **2005**, *2*, 123−160.
(31) Kularatne, S. A.; Venkatesh, C.; Santhapuram, H.-K. R.; Wang, K.; Vaitilingam, B.; Henne, W. A.; Low, P. S. *J. Med. Chem.* **2010**, *53*, 7767−7777.
(32) Frisch, M. J.; Trucks, G. W.; Schlegel, H. B.; Scuseria, G. E.; Robb, M. A.; Cheeseman, J. R.; Scalmani, G.; Barone, V.; Mennucci, B.; Petersson, G. A.; Nakatsuji, H.; Caricato, M.; Li, X.; Hratchian, H. P.; Izmaylov, A. F.; Bloino, J.; Zheng, G.; Sonnenberg, J. L.; Hada, M.; Ehara, M.; Toyota, K.; Fukuda, R.; Hasegawa, J.; Ishida, M.; Nakajima, T.; Honda, Y.; Kitao, O.; Nakai, H.; Vreven, T.; Montgomery, J. A.; Peralta, J. E., Jr.; Ogliaro, F.; Bearpark, M.; Heyd, J. J.; Brothers, E.; Kudin, K. N.; Staroverov, V. N.; Kobayashi, R.; Normand, J.; Raghavachari, K.; Rendell, A.; Burant, J. C.; Iyengar, S. S.; Tomasi, J.; Cossi, M.; Rega, N. J.; Millam, M.; Klene, M.; Knox, J. E.; Cross, J. B.; Bakken, V.; Adamo, C.; Jaramillo, J.; Gomperts, R.; Stratmann, R. E.; Yazyev, O.; Austin, A. J.; Cammi, R.; Pomelli, C.; Ochterski, J. W.; Martin, R. L.; Morokuma, K. V.; Zakrzewski, G.; Voth, G. A.; Salvador, P.; Dannenberg, J. J.; Dapprich, S.; Daniels, A. D.; Farkas, O.; Foresman, J. B.; Ortiz, J. V.; Cioslowski, J.; Fox, D. J. *Gaussian 09*, revision A.02; Gaussian, Inc.: Wallingford, CT, 2009.
(33) Parker, N.; Turk, M. J.; Westrick, E.; Lewis, J. D.; Low, P. S.; Leamon, C. P. *Anal. Biochem.* **2005**, *338*, 284−293.